JACS
JOURNAL OF THE AMERICAN CHEMICAL SOCIETY
Communication
pubs.acs.org/JACS

Magnetically Directed Two-Dimensional Crystallization of OmpF Membrane Proteins in Block Copolymers

Steven S. Klara,[†,▽] Patrick O. Saboe,[‡,▽] Ian T. Sines,[‡] Mahnoush Babaei,[§] Po-Lin Chiu,[∥] Rita DeZorzi,[∥,⊥,○] Kaushik Dayal,[§] Thomas Walz,[∥,⊥,◆] Manish Kumar,[*,‡] and Meagan S. Mauter[*,†,§,#]

[†]Department of Chemical Engineering, Carnegie Mellon University, Pittsburgh, Pennsylvania 15213, United States
[‡]Department of Chemical Engineering, Pennsylvania State University, University Park, Pennsylvania 16802, United States
[§]Deparment of Civil & Environmental Engineering, Carnegie Mellon University, Pittsburgh, Pennsylvania 15213, United States
[∥]Department of Cell Biology, Harvard Medical School, Boston, Massachusetts 02115, United States
[⊥]Howard Hughes Medical Institute, Harvard Medical School, Boston, Massachusetts 02115, United States
[#]Department of Engineering & Public Policy, Carnegie Mellon University, Pittsburgh, Pennsylvania 15213, United States

Supporting Information

ABSTRACT: Two-dimensional (2D) alignment and crystallization of membrane proteins (MPs) is increasingly important in characterizing their three-dimensional (3D) structure, in designing pharmacological agents, and in leveraging MPs for biomimetic devices. Large, highly ordered MP 2D crystals in block copolymer (BCP) matrices are challenging to fabricate, but a facile and scalable technique for aligning and crystallizing MPs in thin-film geometries would rapidly translate into applications. This work introduces a novel method to grow larger and potentially better ordered 2D crystals by performing the crystallization process in the presence of a strong magnetic field. We demonstrate the efficacy of this approach using a β-barrel MP, outer membrane protein F (OmpF), in short-chain polybutadiene-poly(ethylene oxide) (PB−PEO) membranes. Crystals grown in a magnetic field were up to 5 times larger than conventionally grown crystals, and a signal-to-noise (SNR) analysis of diffraction peaks in Fourier transforms of specimens imaged by negative-stain electron microscopy (EM) and cryo-EM showed twice as many high-SNR diffraction peaks, indicating that the magnetic field also improves crystal order.

We present evidence that application of an external magnetic field during the self-assembly of OmpF into 2D crystals increases the size of those crystals. The crystal order also appears to improve. This work represents the first reported instance in which MP 2D crystals in BCPs diffract beyond 1.4 nm resolution.

As perfectly monodisperse nanomaterials with unique transport, sensing, and catalytic properties, MPs are attractive for use in engineered systems. Integration of MPs into short-chain BCP membranes could enhance the robustness of lipid matrix-based MP materials proposed for applications in biosensors,[1] drug delivery,[2] desalination membranes,[3] and energy technologies.[4−6] Today, most investigations into engineered applications of MPs are focused on lipid and BCP vesicle assemblies with low protein packing density.[7−9] Many of these applications would benefit from large crystals (∼10s of microns), the high MP density characteristic for 2D crystals, planar membrane morphology, and tunable, robust supporting materials, such as BCPs.

In addition to applications in engineered systems, 2D BCP-MP crystals may be useful in informing 3D structural models of MPs via electron crystallography. Although MPs are the predominant drug targets,[10] they comprise only 2% of the protein structures in the Protein Data Bank (PDB).[11] A significant barrier to MP structural characterization is the current difficulty in growing highly ordered 2D crystals.[12] Such crystals are extremely useful for characterizing the molecular mechanisms of biological transport, sensing, and signal transduction systems, as well as for designing effective pharmacological agents.[13]

Only one previous study has successfully assembled MPs into 2D crystals within BCP membranes.[14] This earlier study adapted a dialysis-based self-assembly method from the 2D crystallization of MPs in lipid membranes; however, the crystals were small (∼200 nm) and their order was poor (only one order of diffraction spots with a resolution limited to ∼6.5 nm).

A novel approach for improving both short- and long-range order in BCP-MP crystals is to exploit the diamagnetic anisotropy of MPs to impose order on the system during the dialysis-driven crystallization process. All materials in a steady magnetic field have an induced magnetic moment, an intrinsic material property known as diamagnetism. The diamagnetic susceptibility (χ) of a molecule with n identical atoms is given by

$$\chi = \frac{-nZ(\mu_0 e\langle r\rangle)^2}{6m_e}$$

where Z is the atomic number, μ_0 is the magnetic permeability of free space, e is electron charge, m_e is electron mass, and $\langle r\rangle$ is the root-mean-square orbital radius. When the magnetic moment is asymmetric with respect to the three principal axes, χ_1, χ_2, and χ_3, the molecule exhibits diamagnetic anisotropy. Most chemical bonds, including peptide bonds and aromatic rings, exhibit volumetric diamagnetic anisotropies ($\Delta\chi$) on the order of 10^{-18}−10^{-19}.

Received: April 2, 2015
Published: December 17, 2015

DOI: 10.1021/jacs.5b03320
J. Am. Chem. Soc. 2016, 138, 28−31

To obtain the diamagnetic susceptibility tensor for an entire protein, it is necessary to transform the local tensor representation for each bond or small molecule subunit to global coordinates for the protein. To do so, we obtained information on the position and orientation of each MP subunit from the PDB file. We then transformed the tensor representation from local to global coordinates using the second order tensor transformation equation:

$$\chi_i^{\text{global}} = R_i^T \chi_i^{\text{local}} R_i$$

where i refers to the molecular subunit and R_i is the rotation that relates the local and global coordinate systems. The transformed coordinates of each protein subunit were then summed to determine the protein diamagnetic susceptibility:

$$\chi = \sum_i \chi_i^{\text{global}}$$

The protein or oligomer diamagnetic anisotropy, $\Delta\chi$, defined as the difference in the parallel and perpendicular diamagnetic anisotropies, enables comparison between thermal energy, k_BT, and magnetic energy, ΔE, for a protein crystal of N protein or oligomer units:

$$\Delta E = \frac{NV\Delta\chi B^2}{2\mu_o}$$

where V is the unit molecular volume, $\Delta\chi$ is the volumetric diamagnetic anisotropy, B is the magnetic field strength, and μ_o is the permeability of free space. At field strengths or volumes sufficient to satisfy the condition $\Delta E \gg k_BT$, the magnetic field energy dominates and the protein crystal is magnetically stabilized.[15]

While both β-sheet and α-helix structural motifs exhibit strong diamagnetic anisotropy, the tertiary structure of a protein ultimately determines its volumetric diamagnetic anisotropy (Figure 1). For OmpF trimers, this value is approximately -5.5×10^{-7} electromagnetic units (emu). In an applied magnetic field of 7.5 T, a platelet (small 2D crystal) of ~2500 trimers or more will align perpendicular to the direction of the applied field (individual OmpF proteins are aligned parallel to the applied field) and presumably allow further growth of this crystal in the same plane during dialysis. This is effectively equivalent to an OmpF crystal with a minimum dimension of 237 nm. For comparison, a 15 T magnetic field would stabilize a platelet with a minimum dimension of 119 nm. Thus, a larger magnetic field allows growth from smaller crystals leading to more efficient crystallization (see Supporting Information for a detailed analysis

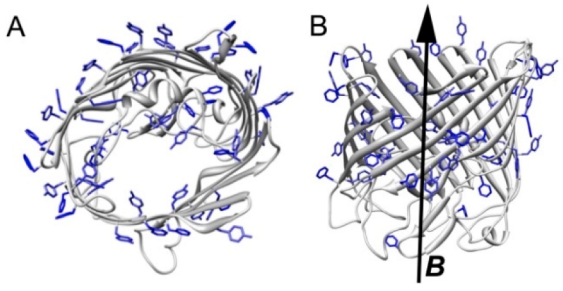

Figure 1. Crystal structure of an OmpF monomer (image created in Chimera[16] with PDB: 2OMF[17]). (A) View down the axis of symmetry of an OmpF trimer. (B) The principal susceptibility and preferred orientation of OmpF in the presence of a magnetic field, B.

with OmpF and the α-helical protein AQP0). The efficacy of high magnetic fields (>1 T) in facilitating 3D crystal formation is well documented,[18,19] but we are unaware of reports of its application to the 2D crystallization of MPs.

The dynamics of self-assembly and the ultimate orientation of MP 2D crystals in the presence of a magnetic field are also influenced by the diamagnetic anisotropy of the supporting BCPs. The alignment of BCPs is a function of the diamagnetic anisotropy of the BCP, the mass fraction of BCP in the final crystal structure, and the thermal fluctuations (kT) of the system. Typically, the mass fraction of BCP in an MP 2D crystal will be less than 10%, and only some of the BCPs used in MP crystal assembly are liquid crystalline.[20] Nevertheless, it may be possible to facilitate improvements to short- and long-range order in MP 2D crystals with very low diamagnetic anisotropy by selecting liquid crystalline BCPs with high diamagnetic anisotropy.

In this work, we test the efficacy of strong magnetic fields in improving short- and long-range order in BCP-MP crystals. *Escherichia coli* OmpF was purified in its native trimeric state and stabilized in detergent solution before reconstitution. Detergent removal through dialysis was used to induce 2D crystallization in the presence and absence of a 7.5 T magnetic field. This crystallization method is an adaptation of techniques developed for 2D crystallization of MPs in lipids[21,22] and BCPs.[14] Although BCPs offer improved chemical stability over lipids,[23,24] the size and order of MP 2D crystals in BCPs were poor in an earlier study. The crystal size was ~0.05 μm^2 and only one order of diffraction spots (corresponding to a resolution of ~7 nm) was visible in Fourier transforms of images of negatively stained samples.[14]

We optimized the dialysis procedure and were able to produce BCP-OmpF crystals comparable in size to those obtained with lipid (~1−10 μm^2) (Figure 2). Of note, compared to the unit cell parameters of OmpF 2D crystals obtained with lipids ($a = b = 7$−15 nm),[25,26] those of crystals obtained with BCPs are larger ($a = b =$ ~19 nm). As the unit cell size varies greatly in 2D crystals obtained in lipids, depending on the lipid, detergent, and method

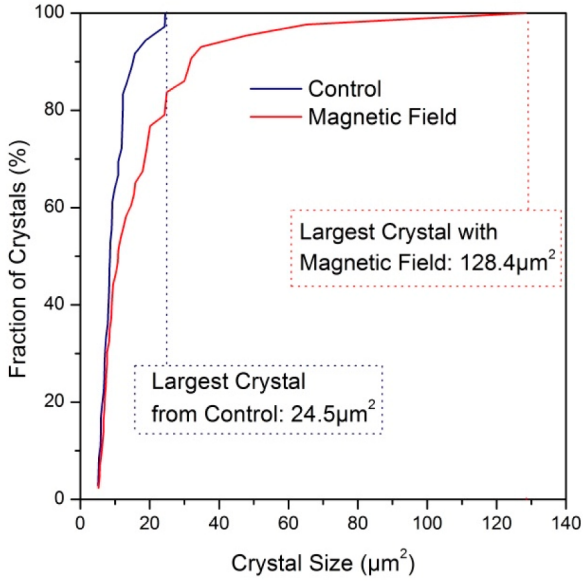

Figure 2. Cumulative distribution function of crystal size for crystals >5 μm^2 from samples crystallized in the absence (control) and presence (magnetic field) of a 7.5 T magnetic field.

DOI: 10.1021/jacs.5b03320
J. Am. Chem. Soc. 2016, 138, 28−31

used for crystallization,[25,26] we hypothesize that different physicochemical properties of the used BCP compared to those of lipids caused OmpF to crystallize with a larger unit cell.

In terms of crystal size, we found that application of an external magnetic field during protein crystallization greatly increased the size of the 2D crystals. The average crystal size was determined through analysis of EM images of negatively stained samples containing 232 crystals with a size of >1 μm^2 using the ImageJ software. The average size of crystals grown in the presence of a magnetic field is larger than that of control crystals, and the largest crystal obtained with a magnetic field is 5 times larger than the largest control crystal (Figure 2 and Supporting Figures 1 and 2).

In addition to increasing crystal size, application of a magnetic field also appeared to increase the order of BCP−OmpF crystals (Figure 3B). We were able to visualize eight orders of diffraction

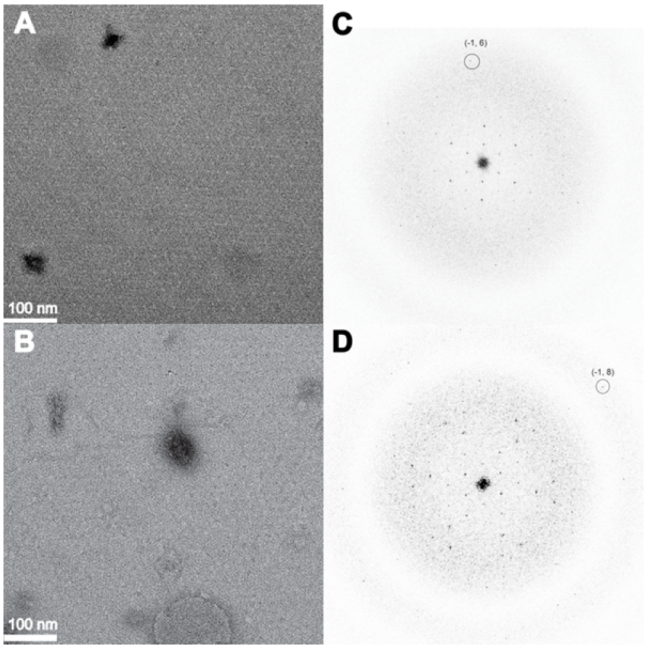

Figure 3. Application of a 7.5 T magnetic field during crystallization appears to enhance the quality of OmpF 2D crystals in BCP membranes. (a,b) Negative-stain EM images of OmpF 2D crystals in PB−PEO membranes assembled by dialysis in the absence (a) and presence (b) of a 7.5 T magnetic field. Scale bars are 100 nm. (c) Fourier transform of a computationally unbent image from a typical OmpF 2D crystal assembled in the absence of a magnetic field. The (−1,6) reflection indicates a resolution of 3.0 nm. (d) Fourier transform of a computationally unbent image from a typical OmpF crystal assembled in the presence of a magnetic field. Samples crystallized in the presence of a magnetic field show an improvement in crystal quality, as evidenced by the (−1,8) reflection that indicates a resolution of 2.2 nm.

spots, corresponding to a resolution of ∼2.2 nm, which is close to the resolution limit imposed by negative staining (Figure 3D).[27] In limited cryo-EM imaging of sugar-embedded crystals prepared by the carbon sandwich technique,[28] we observed up to 12 orders of diffraction in Fourier transforms of crystal images, corresponding to a resolution better than 1.4 nm for aligned samples (see Supporting Figures 3 and 4). The BCP-OmpF crystals exhibited a hexagonal lattice as also seen in the Fourier transforms of the EM images.

In electron crystallography, crystal quality is assessed by evaluating the signal-to-noise ratio of the reflections seen in Fourier transforms of crystal images. The quality of the crystals was analyzed by evaluating the intensity quotient (IQ) plots[29] of reflections in the Fourier transform of unprocessed images. The IQ values in these plots represent the signal-to-noise ratio of the reflections, and reflections that have a higher peak value relative to the background signal have a lower IQ value and can be approximated by the ratio 7(B/A), where A is the amplitude of the diffraction peak (background corrected) and B is the background intensity near the reflection.[30] For reflections with an IQ value of 8 and above, the signal is indistinguishable from the background and is considered noise. Only reflections with IQ values of 5 and below were used for the current analysis.

Table 1 shows the number of reflections with specific IQ values below and above a resolution of 2.4 nm for ten randomly selected

Table 1. Analysis of the Quality of OmpF 2D Crystals Grown in the Presence (Aligned) and Absence (Unaligned) of a Magnetic Field Based on the Signal-to-Noise Ratio of Reflections in Fourier Transforms of EM Images

	average number of reflections[a]			
	aligned		unaligned	
	resolution bins			
IQ[b]	>2.4 nm	≤2.4 nm	>2.4 nm	≤2.4 nm
1	5.6	0.0	2.1	0.0
2	9.2	0.2	6.4	0.2
3	7.0	0.7	5.1	0.5
4	7.9	4.6	5.4	1.6
5	6.0	8.1	5.8	1.6

[a]Standard deviations are provided in Supporting Table 3. [b]The intensity quotient (IQ) is a measure of the signal-to-noise ratio of a reflection in the Fourier transform. The lower the IQ value, the higher the signal compared to the noise.[31]

high quality images of each type. Analysis was conducted on a 0.16 μm^2 randomly selected area on each sample without computational unbending (for one image, IQ spots were analyzed as a function of crystal size, see Supporting Table 2). Samples that were crystallized in the presence of a magnetic field have almost 1.5 times as many high-SNR reflections (IQ values of 1 or 2) than the control samples crystallized in the absence of a magnetic field. Additionally, there is lower variation in the number of high-SNR reflections for the aligned samples compared to the unaligned samples. More reflections were also obtained at higher resolution shells for aligned samples compared to unaligned sample (Table 1). After computational unbending and background subtraction using the *2dx* software,[9] IQ analysis of full-size images reveal twice as many high-SNR reflections for samples crystallized in the magnetic field than the control samples crystallized in the absence of a magnetic field (Supporting Table 3). These high-quality reflections are at higher resolution shells for aligned samples when compared to unaligned samples. An average of 27 high-quality reflections (IQ 1 or 2) were obtained beyond 2.4 nm resolution for aligned samples after computational unbending and background subtraction, while on average only 1.3 such reflections were obtained for the unaligned samples. Although the resolution limit introduced by negative staining and the limited cryo-EM imaging performed hinder our ability to perform a definitive crystallographic analysis, our results strongly indicate that magnetic alignment improves the quality of 2D crystals grown with BCPs.

DOI: 10.1021/jacs.5b03320
J. Am. Chem. Soc. 2016, 138, 28−31

In conclusion, we demonstrate that exploiting the diamagnetic anisotropy of molecular bonds within the MP structure can significantly increase the size of BCP-MP 2D crystals and also appears to improve the order of the crystals.

■ ASSOCIATED CONTENT

Supporting Information

The Supporting Information is available free of charge on the ACS Publications website at DOI: 10.1021/jacs.5b03320.

Experimental methods and procedures, materials information, and image characterization (PDF)

■ AUTHOR INFORMATION

Corresponding Authors

*manish.kumar@psu.edu

*mauter@cmu.edu

Present Addresses

○Dipartimento di Scienze Chimiche e Farmaceutiche, Trieste 34127, Italy.

◆The Rockefeller University, New York, New York 10065, United States.

Author Contributions

▽These authors contributed equally to this work.

Notes

The authors declare no competing financial interest.

■ ACKNOWLEDGMENTS

S.K. was supported by the US National Science Foundation (NSF) Nanotechnology Environmental Effects and Policy Integrated Graduate Education and Research Traineeship (DGE-0966227). Access to magnets was kindly provided by the Pittsburgh NMR Center for Biomedical Research, which is funded by a grant from the National Institute of Biomedical Imaging and Bioengineering (NIBIB) as a Biomedical Technology Research Center (P41 EB001977). M.B. and K.D. thank ONR Applied and Computational Analysis (N00014-14-1-0715) for support. Research at Penn State was funded in part by the United States Environmental Protection Agency (EPA) under the Science to Achieve Results (STAR) Graduate Fellowship Program. EPA has not officially endorsed this publication and the views expressed herein may not reflect the views of the EPA. The Shared Fermentation Facility (SFF) at Penn State provided access to bioreactor and cell processing equipment. Penn State undergraduates and REU students Payton Forrest, Samantha Summers, Zach Jansma, and Sean McCrea as well as by Gianmarco Terrones from the Potomac High School are also acknowledged.

■ REFERENCES

(1) Vamvakaki, V.; Chaniotakis, N. A. *Biosens. Bioelectron.* **2007**, *22*, 2848−2853.

(2) Onaca, O.; Enea, R.; Hughes, D. W.; Meier, W. *Macromol. Biosci.* **2009**, *9*, 129−139.

(3) Kumar, M.; Grzelakowski, M.; Zilles, J.; Clark, M.; Meier, W. *Proc. Natl. Acad. Sci. U. S. A.* **2007**, *104*, 20719−207243.

(4) Grimme, R. A.; Lubner, C. E.; Golbeck, J. H. *Dalton Trans.* **2009**, 10106−10113.

(5) Saboe, P. O.; Lubner, C. E.; McCool, N. S.; Vargas-Barbosa, N. M.; Yan, H.; Chan, S.; Ferlez, B.; Bazan, G. C.; Golbeck, J. H.; Kumar, M. *Adv. Mater.* **2014**, *26*, 7064−7069.

(6) Badura, A.; Kothe, T.; Schuhmann, W.; Rögner, M. *Energy Environ. Sci.* **2011**, *4*, 3263−3274.

(7) Ho, D.; Chu, B.; Lee, H.; Montemagno, C. D. *Nanotechnology* **2004**, *15*, 1084−1094.

(8) González-Pérez, A.; Stibius, K. B.; Vissing, T.; Nielsen, C. H.; Mouritsen, O. G. *Langmuir* **2009**, *25*, 10447−10450.

(9) Shen, Y.-x.; Saboe, P. O.; Sines, I. T.; Erbakan, M.; Kumar, M. *J. Membr. Sci.* **2014**, *454*, 359−381.

(10) Arinaminpathy, Y.; Khurana, E.; Engelman, D. M.; Gerstein, M. B. *Drug Discovery Today* **2009**, *14*, 1130−1135.

(11) Pogozheva, I. D.; Tristram-Nagle, S.; Mosberg, H. I.; Lomize, A. L. *Biochim. Biophys. Acta, Biomembr.* **2013**, *1828*, 2592−2608.

(12) Hankamer, B.; Glaeser, R.; Stahlberg, H. *J. Struct. Biol.* **2007**, *160*, 263−264.

(13) Hopf, T. A.; Colwell, L. J.; Sheridan, R.; Rost, B.; Sander, C.; Marks, D. S. *Cell* **2012**, *149*, 1607−1621.

(14) Kumar, M.; Habel, J. E. O.; Shen, Y.; Meier, W. P.; Walz, T. *J. Am. Chem. Soc.* **2012**, *134*, 18631−18637.

(15) Worcester, D. *Proc. Natl. Acad. Sci. U. S. A.* **1978**, *75*, 5475−5477.

(16) Pettersen, E. F.; Goddard, T. D.; Huang, C. C.; Couch, G. S.; Greenblatt, D. M.; Meng, E. C.; Ferrin, T. E. *J. Comput. Chem.* **2004**, *25*, 1605−1612.

(17) Cowan, S.; Garavito, R.; Jansonius, J.; Jenkins, J.; Karlsson, R.; König, N.; Pai, E.; Pauptit, R.; Rizkallah, P.; Rosenbusch, J. *Structure* **1995**, *3*, 1041−1050.

(18) Sazaki, G. *Prog. Biophys. Mol. Biol.* **2009**, *101*, 45−55.

(19) Numoto, N.; Shimizu, K.-i.; Matsumoto, K.; Miki, K.; Kita, A. *J. Cryst. Growth* **2013**, *367*, 53−56.

(20) Nardin, C.; Hirt, T.; Leukel, J.; Meier, W. *Langmuir* **2000**, *16*, 1035−1041.

(21) Raunser, S.; Walz, T. *Annu. Rev. Biophys.* **2009**, *38*, 89−105.

(22) Jap, B.; Zulauf, M.; Scheybani, T.; Hefti, A.; Baumeister, W.; Aebi, U.; Engel, A. *Ultramicroscopy* **1992**, *46*, 45−84.

(23) Lee, J. C. M.; Bermudez, H.; Discher, B. M.; Sheehan, M. A.; Won, Y. Y.; Bates, F. S.; Discher, D. E. *Biotechnol. Bioeng.* **2001**, *73*, 135−145.

(24) Grit, M.; Crommelin, D. J. *Chem. Phys. Lipids* **1993**, *64*, 3−18.

(25) Glaeser, R. M.; Downing, K.; DeRosier, D.; Chiu, W.; Frank, J. *Electron Crystallography of Biological Macromolecules*; Oxford University Press, 2007.

(26) Hoenger, A.; Gross, H.; Aebi, U.; Engel, A. *J. Struct. Biol.* **1990**, *103*, 185−195.

(27) Ohi, M.; Li, Y.; Cheng, Y.; Walz, T. *Biol. Proced. Online* **2004**, *6*, 23−34.

(28) Gyobu, N.; Tani, K.; Hiroaki, Y.; Kamegawa, A.; Mitsuoka, K.; Fujiyoshi, Y. *J. Struct. Biol.* **2004**, *146*, 325−333.

(29) Henderson, R.; Baldwin, J. M.; Downing, K. H.; Lepault, J.; Zemlin, F. *Ultramicroscopy* **1986**, *19*, 147−178.

(30) Henderson, R.; Baldwin, J. M.; Ceska, T. A.; Zemlin, F.; Beckmann, E.; Downing, K. H. *J. Mol. Biol.* **1990**, *213*, 899−929.

(31) Gipson, B.; Zeng, X.; Zhang, Z. Y.; Stahlberg, H. *J. Struct. Biol.* **2007**, *157*, 64−72.

DOI: 10.1021/jacs.5b03320
J. Am. Chem. Soc. 2016, 138, 28−31